
CHANGING SPEED IN A SIMPLE WALKER WITH DYNAMIC ONE-STEP TRANSITIONS

by L.H.F van Zijl

MASTER THESIS

SEPTEMBER 5, 2009

Preface

In this thesis I describe the main part of the research I did at the Delft Biorobotics Lab to finish my master in BioMechanical Engineering at the 3ME faculty of the Delft University of Technology. This report is set up in the form of an article that is going to be submitted to the International Journal of Humanoid Robots. Co-author on this article is Dr. S.H. Collins, who was my supervisor during this research. Hopefully my report contributes to the ongoing research in the field of Dynamic Walking. It was a great experience to work on a subject that could be of importance in the future of both medical as well as personal assisting devices in the inspiring environment of the Delft Biorobotics Lab.

I would like to thank Steve Collins for his supervision and contribution during my research and Martijn Wisse and the members of the Delft Biorobotics Lab for sharing thoughts, interesting discussions and a great time.

CHANGING SPEED IN A SIMPLE WALKER WITH DYNAMIC ONE-STEP TRANSITIONS

L. H. F. VAN ZIJL and S. H. COLLINS

*Delft Biorobotics Lab,
Department of Mechanical Engineering, Delft University of Technology,
Mekelweg 2, 2628CD Delft, The Netherlands
l.h.f.vanzijl@student.tudelft.nl*

In this study we try to improve versatility of dynamic walkers by proposing a strategy to make walking speed transitions in a simple powered 2D walking model. Earlier studies on this subject succeeded in convergence towards a desired speed, but we apply control inputs that are calculated beforehand, to perform one step starting from a certain speed and ending in such a configuration to continue walking at the desired new speed. We show that such “Dynamic One-Step Transitions”, can be applied to starting, speeding up, slowing down and stopping, to make a big velocity change within one step. A parameter study evaluating energy use and disturbance rejection showed that energy is best to be added by a push-off and that a torso torque should only be applied when necessary to initiate a starting transition or to dissipate energy to slow down or stop. For disturbance rejection evaluation we proposed several measures, which all showed similar trends in predicting actual disturbance rejection. The best disturbance rejection for the transition is obtained when the swing leg actuation results in swing leg retraction. With this research we have shown that versatility of dynamic walkers can be improved with walking speed transitions, still exploiting the natural dynamics of the system.

Keywords: Dynamic one-step transition; walking speed; dynamic walking.

1. Introduction

Humanoid robots are foreseen to be future assisting devices for example in health care. To realize this goal, one function to fulfill is to move around and one manner to do so is to walk. Two approaches can be recognized within research on walking, the so-called ZMP approach, applying trajectory control^{1,2}, and the dynamic walking approach, based on passive dynamics³. Trajectory controlled humanoids have demonstrated impressive results on walking and versatility, but when research on human walking is compared to mechanical models then dynamic walkers show the best resemblance on both the human like appearance of the motion as well as energy efficiency and control properties⁴. Therefore dynamic walking, or limit cycle walking⁵, is a very promising strategy to be useful for both studies on humanoid robotics as well as human walking. One of the things that have to be improved on dynamic walkers is their versatility and one aspect of versatility is the ability to change speed while walking.

Little research has been done on changing walking speed in the field of dynamic walking. Mandersloot et al.⁶ applied dynamic programming to optimize energy use while controlling walking speed. Hobbelen and Wisse⁷ applied a combination of feedforward and feedback to control the walking speed. But the wanted speed was always obtained after several steps of convergence towards it. And the effect of a walking speed transition on the disturbance rejection of the walker has not been investigated in none of both of the studies.

We propose that it might be possible to change the walking speed of a dynamic walker by making one transition step with changed control input values. This would result in a “Dynamic One-Step Transition” between two known cyclic motions with different speeds. The fact that such a dynamic one-step transition is based on dynamic walking principles by using the natural dynamics of the system implies that the advantage of high efficiency of dynamic walking would also apply to our transition. The needed actuation values are to be calculated on forehand and no trajectory control would be applied. This differs from existing research on velocity transitions where feedback laws are applied to converge towards the desired speed within several steps⁷.

Our proposed approach requires a method to find the needed control input values for such a transition to investigate whether there exist trends for the control input values to follow, in order to result in an ideal transition step in terms of energy use and disturbance rejection. This could improve dynamic walkers versatility and improve understanding of how humans perform such transitions.

While evaluating the disturbance rejection during a transition, we have to be aware of the fact that we can not apply existing stability qualification measures based on cyclic stability, because a walking speed transition is not a cyclic motion. And also we are not interested in local stability in terms of local convergence to a trajectory. For these two reasons we will totally avoid the term “stability”. But in order to optimize the fall-avoidance capacities of the walker making a transition, we do focus on disturbance rejection. We evaluate different potential measures to quantify disturbance rejection of the transition, which can be subdivided into *Targeting* and *Robustness* measures.

We use a model based on the simplest walker⁸ for which it is easy to demonstrate the basics of limit cycle walking, utilizing the natural dynamics of the system, and its advantages, because of the simplicity of this model. This allows us to show that our strategy to transition also exploits the benefits of limit cycle walking in terms of its efficiency and self-stabilizing properties. Four control inputs are added to the model to walk on level ground, and to initiate different types of transitions. To find the needed control input values for a transition we applied a gradient descent search. We evaluated the resulting transition steps on their energy use and disturbance rejection. The results are used to evaluate both the method in general as well as to distinguish specific strategies for specific types of transitions. We also applied discrete optimal control to the transition in order to achieve even better disturbance rejection.

2. Model and Methods

We applied a model based approach, using the simplest walking model⁸ extended with control inputs to initiate several kinds of transitions while walking on level ground. We applied a gradient descent search method to find the values for the control inputs for a transition. Resulting combinations of values for the control inputs were evaluated on their energy use, in terms of mechanical work. We devised new disturbance rejection quantification measures to also evaluate the disturbance rejection capabilities of the walker making transitions. Finally we applied discrete optimal control to improve the disturbance rejection properties.

2.1. Model description

Our model is based on the simplest walking model⁸, consisting of two massless legs, a point-mass at the hip and infinitesimal point-masses at the feet. The legs were modeled as a double pendulum, hinged at the hip and hinged at the stance foot connecting the model with the ground. The angle of the stance-leg θ is measured with the normal to the ground, the angle of the swing leg ϕ is measured with respect to the stance leg, as shown in figure 1. The angles and their angular velocities represent the generalized coordinates of the system. The model walks on level ground. The feet have plastic collisions with the walking surface.

To compensate for the energy loss at foot-strike, energy can be added to the system by a push-off impulse P instantaneously before foot-strike and by a constant torque τ_{torso} between the stance leg and a virtual torso with zero mass and infinite moment of inertia. The motion of the swing leg is determined by the motion of the hip, and two separate actuators, a torque caused by a torsion spring with stiffness K_p and an constant applied torque, τ_{swing} .

The model as described led to the equations of motion^{8,9} expanded with the extra actuation parameters τ_{torso} and τ_{swing} (1, 2). With hip mass $M = 1$ and leg length $l = 1$ and time scaled by a factor $\sqrt{l/g}$, the equations of motion are expressed in dimensionless terms:

$$\ddot{\theta} = \sin(\theta) - \tau_{torso} \quad (1)$$

$$\ddot{\phi} = \ddot{\theta} + \sin(\phi) \left(\dot{\theta}^2 - \cos(\theta) \right) - K_p \phi - \tau_{swing} \quad (2)$$

This results in dimensionless terms for other quantities like velocity as well as energies¹⁰. When the heel strike event $\phi = 2\theta$ is detected, the time continuous swing phase ends and the swing leg becomes the stance leg and vice versa. This results in an instantaneous shift of the angles and angular velocities before collision towards the angles and angular velocities after collision. The states after impact are calculated using conservation of angular momentum and impulse-momentum equation and the effect of the impulse^{8,9}. Observing the walker on a step-to-step basis, we considered one step as a function of the states at the beginning of a step

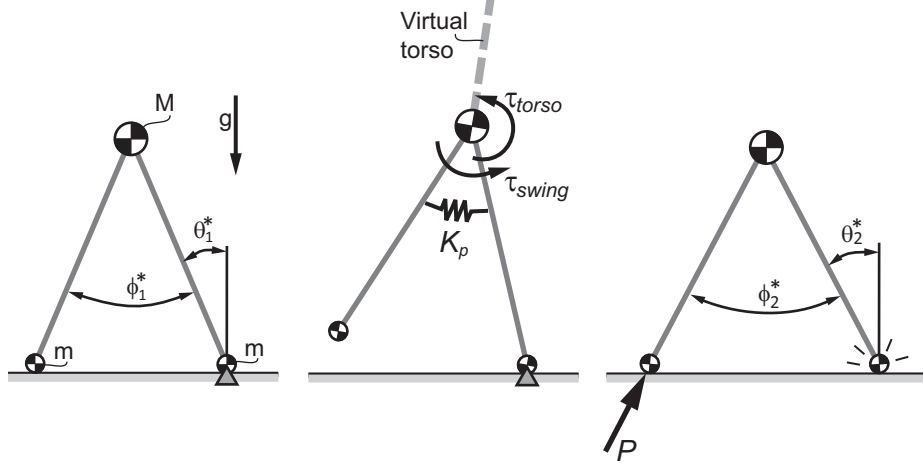


Fig. 1: The simple powered walking model making a transition step, starting with angles and angular velocities from the first fixed point \mathbf{x}_1^* . During every step the walker is actuated by a torque τ_{torso} between a virtual torso and the stance leg, a torque τ_{swing} between the stance leg and the swing leg, and a linear torsional spring with stiffness K_p . At the end of the step a push-off P is applied just before collision and the step to step transition. A transition step ends with the angles and angular velocities of the second fixed point \mathbf{x}_2^*

(\mathbf{x}_n) and the values for the control inputs (\mathbf{u}_n), to the states at the beginning of the next step (\mathbf{x}_{n+1}):

$$\mathbf{x}_{n+1} = S(\mathbf{x}_n, \mathbf{u}_n) \quad (3)$$

This function S is defined by the equations of motion and the step-to-step transition including the instantaneous push-off. With certain values for the control inputs in \mathbf{u}_n and proper initial conditions in \mathbf{x}_n , the dynamics of the system result in a periodic motion where the state at the beginning of each step is equal to the state at the beginning of the next step, as in:

$$\mathbf{x}^* = S(\mathbf{x}^*, \mathbf{u}^*) \quad (4)$$

The repeating states \mathbf{x}^* are called fixed points. We investigated speed transitions between three different fixed points, one for standing still and two for slow and normal speed walking. The angles and angular velocities in the fixed points were based on step frequency and step length relations preferred by humans^{11,12}. Corresponding control input values were chosen such that they resulted in low energy use⁹ and good disturbance rejection by applying swing leg retraction^{13,14}. In figure

2 the limit cycles and fixed points are shown, belonging to slow and normal walking, as well as standing still with both legs next to each other.

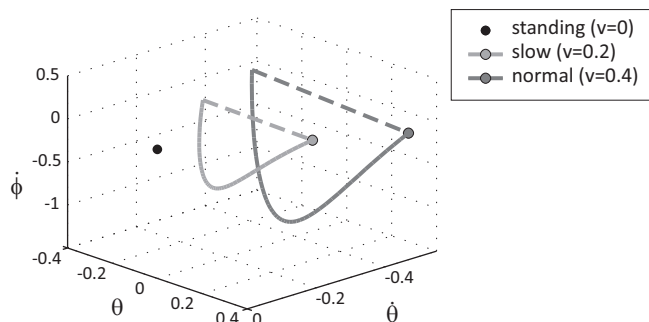


Fig. 2: The fixed points and corresponding limit cycles that are investigated are shown in phase space. The effect of the collision is shown by a dashed line. The single dot represents the states when standing still.

The step-length and velocity relations are shown in table 1. Both normalized dimensionless velocities (Froude number Fr) and in SI units are shown, which are related as in $Fr = \frac{v}{\sqrt{gl}}$.

Table 1: Fixed points and their settings. Speed v , step length L_s and step frequency F_s are given in SI units and dimensionless. In the middle part the angles and angular velocities of both legs are given at the fixed point. In the right part the values for the control inputs are given.

	Gait parameters						Fixed point states				Control inputs			
	v [ms^{-1}]	L_s [m]	F_s [s^{-1}]	v [-]	L_s [-]	F_s [-]	θ^* [rad]	ϕ^* [rad]	$\dot{(\theta)}^*$ [rad]	$\dot{\phi}^*$ [rad]	P [-]	τ_{torso} [-]	K_p [-]	τ_{swing} [-]
stand	0	0	0	0	0	0	0	0	0	0				
slow	0.63	0.48	1.30	0.2	0.48	0.42	0.244	0.488	-0.291	-0.034	0.073	0	1.10	0.0037
normal	1.25	0.68	1.84	0.4	0.68	0.59	0.348	0.697	-0.502	-0.117	0.182	0	2.85	0.0067

2.2. Finding transition control inputs

A walking speed transition could be made in one dynamic walking step, with control input values calculated beforehand, starting with the initial conditions (angles and angular velocities) of the first walking cycle (fixed point \mathbf{x}_1^*) and ending with the initial conditions for the second walking cycle (fixed point \mathbf{x}_2^*).

We applied the gradient descent search method to find the needed values for the control inputs for a transition. This method has been applied by others to find fixed points for steady state walking^{3,9}. In a search for transition control input values it could be applied by minimizing to zero the Euclidean distance between the end of the transition step and the goal fixed point, as in:

$$\|\mathbf{e}\| = \|S(\mathbf{x}_1^*, \mathbf{u}_T) - \mathbf{x}_2^*\| \quad (5)$$

The minimum of this function is found by iteratively adapting the values for the control inputs of the transition step \mathbf{u}_T by:

$$\Delta \mathbf{u}_T = -J^{-1} \mathbf{e} \quad \text{with} \quad J = \frac{\partial \mathbf{e}_i}{\partial u_j} \quad (6)$$

The Jacobian J represents the changes in the error \mathbf{e} when the control input values are independently varied within the linear region around the original settings. All possible steps in the gradient descent search are shown in figure 3.

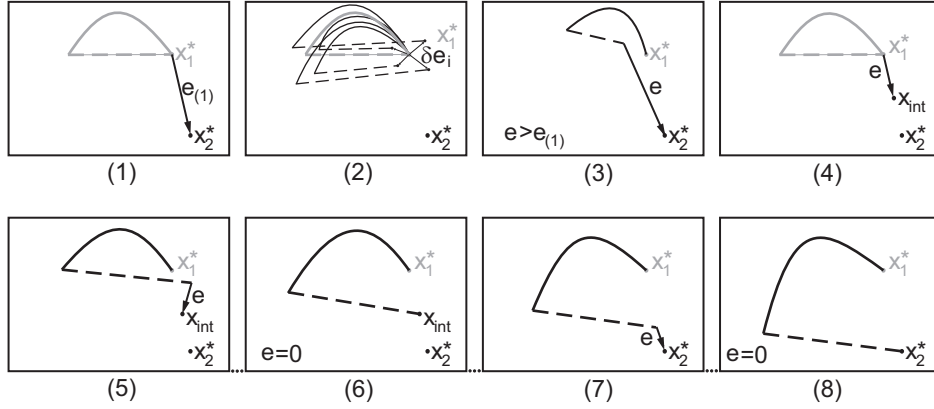


Fig. 3: Finding transition step parameters using a gradient search: 1. Initial error equal to the distance between \mathbf{x}_1^* and \mathbf{x}_2^* ; 2. build the Jacobian J ; 3. the new input values are calculated with $\Delta \mathbf{u} = -J^{-1} \mathbf{e}$. Applying calculated \mathbf{u} can result in a bigger error and no convergence; 4. then try search for intermediate point first; 5. converge toward the intermediate point (not shown: if not converging, try new intermediate point closer to \mathbf{x}_1^*); 6 adjusting input values again finally results in a transition step to the intermediate point; 7. adjusting input values again (several times), results in the wanted transition step. Between step 4, 5, 6, 7 and 8 new Jacobian's and $\Delta \mathbf{u}$ are calculated analogous as shown in step 2.

It is possible that a transition between two fixed points could be performed with

multiple parameter combinations. This would leave room for optimization in terms of energy use and disturbance rejection, which was the case in our model.

2.3. Energy use

We measured energy use of transition steps in terms of mechanical work done by the control inputs and determined the transition that resulted in lowest energy use. The energy added by push-off for this model is equal to half the square of the push-off magnitude⁹. The work done by the other actuators is equal to the integral of the angular velocity times the torque from the actuator over time. The work done by the actuation of the stance leg and the hip mass (P and τ_{torso}) can be separated from the work done by the swing leg actuation (K_p and τ_{swing}), because of the fact that the legs and feet are massless. This results in:

$$E_{stance} = \frac{1}{2}P^2 + \int |\tau_{torso}\dot{\theta}|dt \quad (7)$$

$$E_{swing} = \int |K_p\phi\dot{\phi}|dt + \int |\tau_{swing}\dot{\phi}|dt \quad (8)$$

In spite of the fact that both the spring and τ_{swing} act on a massless leg, the energy use of this actuation is still evaluated by comparing the work done. Real robots and humans do not have massless legs and therefore this energy use calculation is relevant.

2.4. Disturbance Rejection

We evaluated the disturbance rejection capacities of the walker making transitions and determined which parameter combination resulted in highest disturbance rejection. But existing disturbance rejection measures from steady state walking were not applicable to transitions, because they are not cyclic motions. Therefore we set up a list of possible disturbance rejection quantification measures that can be applied to transitions. The first set of measures were computed from the transition step only and we will refer to them as “targeting” measures, because they focus on how close the transition step ends near the goal fixed point expressed in distance, mechanical energy or convergence (to a non-consistent reference point). These targeting measures were easy and fast to compute, but the fact that they focus on the transition only is also a disadvantage, because whether a walker would fall after a perturbed transition step highly depends on the stability of the goal fixed point. A complementary set of measures, the “robustness” measures, determine the disturbance rejection capabilities from the transition step and proceeding steps. These measures needed more computation time, but they should have better correlation with the actual fall-avoidance properties of the walker performing a transition. We compared results from the targeting and robustness measures to a measure that represents a good estimate of the disturbance rejection of a walker in an environment comparable to the real-world, but is very difficult to compute:

- *Actual disturbance rejection* was computed as the magnitude of a combination of two Gaussian white noise disturbances for which the walker is able to prevent falling in 95% of the cases during 60 trials consisting of 5 steps before transition, one transition step and 10 steps after the transition. The disturbances were pushes and floor irregularities.

Targeting measures are based on the idea that in general the smaller the deviation from the goal fixed point at the end of a transition step $\Delta\mathbf{x}$, the better. Therefore we use the following targeting measures to find an expression for this deviation after a transition that started with perturbed initial conditions and/or was disturbed during the transition. The reciprocal of the measures is taken to compare their results with the actual disturbance rejection:

- *Deviation measure* defined as $\|\Delta\mathbf{x}\|^{-1}$ directly focuses on the Euclidean distance to the goal fixed point, at the end of a perturbed transition step. This measure is fast to compute and can be used to evaluate the response of the walker to disturbances both during as well as prior to the transition step. It does not give information on the direction of the deviation from the goal fixed point in phase space, which is a disadvantage because the rate of convergence to the goal fixed point is not equal in all directions.
- *Energy difference measure.* A deviation from the goal fixed point could correspond with a configuration (angles and angular velocities) that has almost the same mechanical energy as the configuration of the fixed point. Another deviation in another direction in phase space could correspond with a configuration with a big energy difference with the configuration of the fixed point. If the first deviation has a less negative effect on the following steps than the second, then expressing the deviation from the goal fixed point in terms of difference in mechanical energy, $|\Delta E|^{-1} = |E(\mathbf{x}^*) - E(\mathbf{x})|^{-1}$, would combine some information about the direction as well as the magnitude of the deviation into one value. This measure is easy and fast to compute, but there exists no proof that the difference in energy gives a good indication of the effect of a disturbance.
- *Eigenvalues* The eigenvalues of the linearized step function of a transition step would indicate rate of growth or decay by comparing the deviation from two different fixed points (the starting fixed point and the goal fixed point). Because of the fact that distances to two different fixed points are being compared, this can not be used to qualify stability. But in general we can state that the closer the eigenvalues to zero, the better. For that reason we could use the reciprocal of the maximal eigenvalue, $(\max \|eig\|)^{-1}$ of the linearized transition step function to quantify the targeting capacity of the transition. This measure only indicates rate of convergence during the transition step, after disturbances taking place before the transition step, and not during the transition step. The eigenvalues are an often used measure for stability in steady state walking even though the correlation

with the actual disturbance rejection for steady state walking has been shown to be low¹⁵.

Our robustness measures focus on the transition step and the following steps. When the properties of the goal fixed point are remained the same and only the settings of the transition are changed, then the changes in the proceeding steps are a direct response to a perturbation before or during the transition. By examining the proceeding steps one could see whether the likelihood of falling after the transition increases when a control input for the transition step had been changed. This implies that the robustness measures need more computing time than targeting measures, because both the transition step as well as a set of proceeding steps have to be simulated.

- The *Gait Sensitivity Norm*¹⁵ can be used to measure the effect of a perturbation e before or during the transition step on the gait indicator g , of the transition step ($n = 0$) and during steady state gait after the transition ($n = 1..∞$), as in:

$$\left\| \frac{\partial g}{\partial e} \right\|_2 = \frac{1}{|e_0|} \sqrt{\sum_{n=0}^{\infty} (g_n - g^*)^2} \quad (9)$$

The perturbation e is a combination of a step down and a push back disturbance. Step time was chosen to be the gait indicator g , because it has proven to be a reliable gait indicator in the case of steady state walking. The GSN measures the response to a fixed disturbance, and takes therefore one simulation of a sequence of a transition step and the following steps. This could be computed reasonably fast. And the correlation of the GSN with the actual disturbance rejection is high in the case of steady state walking¹⁵, which could also be expected to hold for transitions. For this measure holds that lower is better, therefore the reciprocal, GSN^{-1} , was taken to enable comparison with the actual disturbance rejection.

- The *Maximum allowable deterministic disturbance*, $max|e|$, is the maximum disturbance magnitude for which the walker will not fall within a certain amount of not disturbed steps through the second fixed point after the transition, when exposed to a disturbance before or during the transition. This could be a single disturbance (step-down, step-up, push forward or push backward), but we evaluated a combination of a floor irregularity and push. The fact that the sequence of a transition step and its proceeding steps had to be computed multiple times until the $max|e|$ was known, is a disadvantage.

2.5. Simulation

We computed the energy use and disturbance rejection for every combination of control input values that resulted in the wanted transition to compare parameter

settings for the four types of transitions. The settings of the fixed points were never changed, to ensure that all observed changes were due to changes in the transitions. The investigated disturbance rejection measures were computed for a combination of a step down and push back disturbance, because they are both considered regular occurring disturbances from the real world, where a step down adds energy and a push back takes energy from the system. The magnitude of the step down and push back are always kept equal to each other. For the computation of $\|\Delta\mathbf{x}_{n+1}\|$, $|\Delta E_{n+1}|$ and GSN they were set to 0.001. The eigenvalues are independent of the disturbance type. For the disturbance rejection computation for the starting transition, the disturbances took place during the transition step. For the speeding up, slowing down and stopping transition, the walker was exposed to the disturbances during the step prior to the transition step. The GSN , $max|e|$ and actual disturbance rejection were not computed for the stopping transition, due to the fact that there are no steps after the stopping transition.

2.6. Improving disturbance rejection with state-feedback

When a disturbance occurs during the walking cycles prior to the transition step, they will cause the walker to deviate from the first fixed point, causing the transition step to start with perturbed initial conditions. In an attempt to minimize the effect of such a perturbation, we tested the effect of applying Discrete LQR control in the form of: $\Delta\mathbf{x}_{n+1} = (\mathbf{A} - \mathbf{BK})\Delta\mathbf{x}_n$. The linearized step function \mathbf{A} describes the effect of perturbed initial conditions on the end of the step. Control authority matrix \mathbf{B} is the derivative of the linearized step to input changes $\Delta\mathbf{u}$. The gain matrix \mathbf{K} is build such that it minimizes the cost function of error ($\Delta\mathbf{x}_{n+1}$) and effort ($\Delta\mathbf{u}$). When DLQR was applied, it was applied to both the walking cycles as well as to the transition.

3. Results

We succeeded in applying the dynamic one-step transition strategy to all four types of transitions of interest. This transition strategy could also be applied to transitions with much bigger velocity differences then ones investigated. We found that the less energy is used for starting and speeding up when all or almost all energy is put in by push-off. We also found that for slowing down and stopping, the transitions performed without push-off P used lowest energy. Additionally, comparison of the results of different disturbance rejection measures to the actual disturbance rejection indicated that all measures showed more or less the same trends for varying control input values. Focusing on disturbance rejection, we found that there exists a region of possible combinations of push-off P and torque τ_{torso} that could result in a transition that had high disturbance rejection, if a good combination of stiffness K_p and torque τ_{swing} was chosen. Also in this section it is shown that there exists an optimal combination of K_p and τ_{swing} that can be found using our disturbance rejection measures.

3.1. Transition results

We were able to perform all four transitions of interest by applying control input values found by the gradient descent search method to the dynamic one-step transition strategy. In figure 4 solutions are shown for every transition.

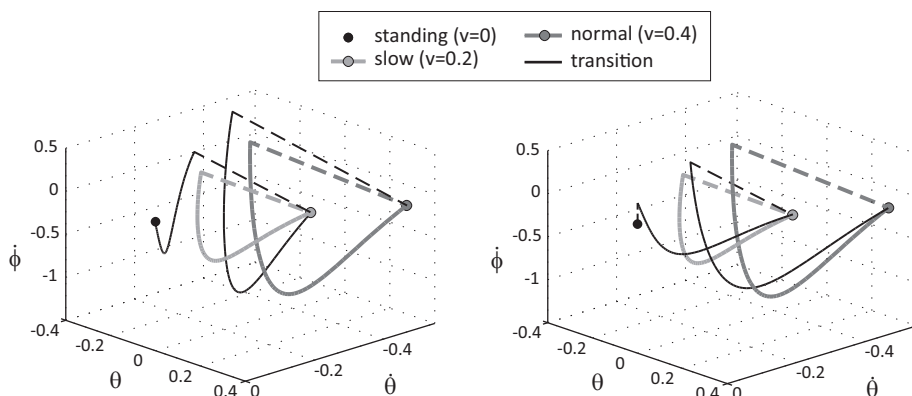


Fig. 4: Solutions for the intended transitions. On the left for starting and speeding up transitions and on the right solutions for slowing down and stopping transitions. The effect of the collision is shown by a dashed line.

While exploring the applicability of our transition strategy, the same type of transitions could be made with much larger speed changes within one step. For starting (from zero velocity) and also speeding up (from a velocity of 0.2), it was possible with our model to make a dynamic one-step transition changing the speed to a dimensionless speed of 1.3 (equivalent to 4 m s^{-1}) which is about two times the human preferred walk-to-run transition speed of about 0.64 (2 m s^{-1}). The same holds for slowing down and stopping, where it was possible to slow down from a dimensionless speed of 1.3 to 0.2 and zero respectively.

3.2. Energy Use Results

For a transition between two fixed points, the choice of the control input values affected the energy use. In figure 5 the energy input from push-off P and τ_{torso} are plotted for every value for P that gave a solution and its corresponding value for τ_{torso} for three types of transitions.

For starting and speeding up, the lowest energy use is shown in the region where the amount of torque τ_{torso} was close to zero and zero respectively. For both cases the minimum energy use approaches the mechanical energy difference between the states of the fixed points before and after the transition, which are 0.0129 for starting and 0.053 for speeding up. For slowing down, the control input values choice that led

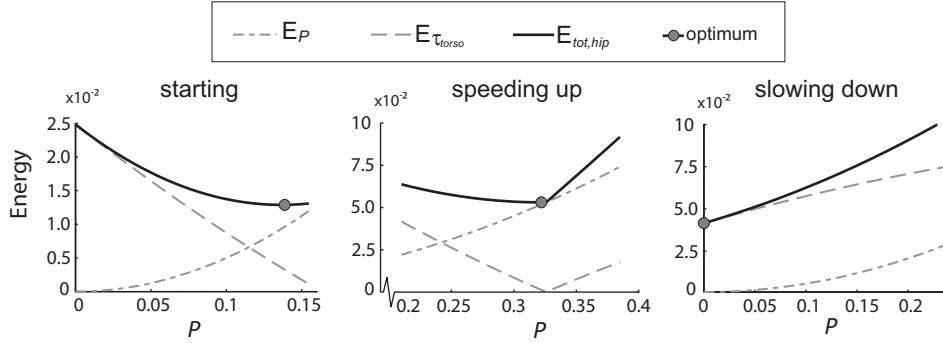


Fig. 5: Plots of amount of push-off P versus energy added to the hipmass for, starting, speeding up and slowing down. The stopping transition can only be done with $P = 0$, resulting in an energy use of 0.0129. Therefore no plot is shown for this transition.

to lowest energy use was such that no energy is put in by push-off P . The stopping transition could only be made with push-off set to zero. For these two transitions the amount of energy that has to be dissipated is 0.053 and 0.0129 respectively, which is done by the torso torque almost completely for slowing down and completely for stopping.

In figure 6 the energy use caused by the spring and the swing leg torque is shown, in the case of the optimal push-off P and torso torque τ_{torso} relation for every transition. The results indicate that the lowest possible stiffness K_p for which a solution could be found for the transition, resulted in the lowest energy use by the actuation of the swing leg. We examined the energy use for other P and τ_{torso} too and found the same trends.

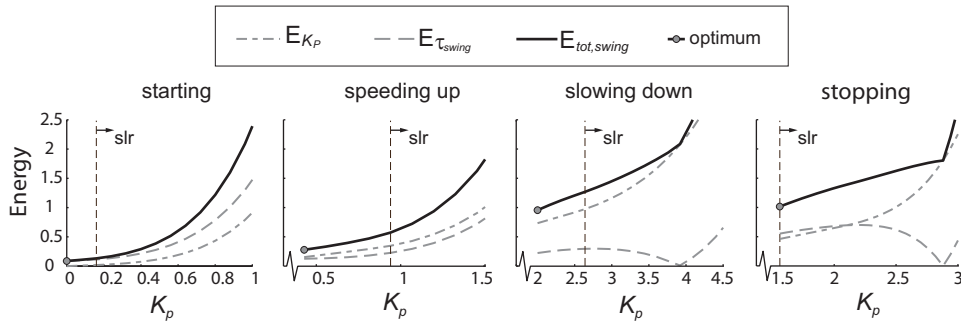


Fig. 6: Plots of spring stiffness K_p versus work done by the actuators on the swing leg for starting, speeding up, slowing down and stopping. Settings on the right of the vertical dashed line result in swing leg retraction (slr).

3.3. Disturbance Rejection results

When comparing the results from the proposed targeting and robustness measures with the results on actual disturbance rejection, we noticed that all measures showed similar trends. This is shown in figure 7, where the results are plot for variable stiffness K_p for the speeding up transition.

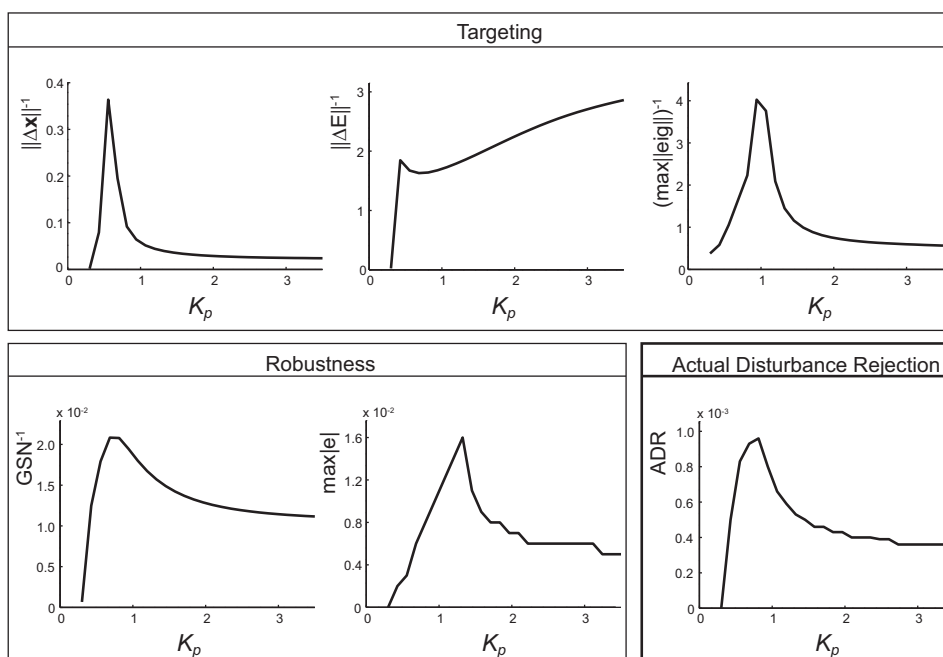


Fig. 7: Plots of results of K_p value versus targeting and robustness measures, compared to the actual disturbance rejection for the speeding up transition. The values push-off P and τ_{torso} are the same for every plot, and chosen such that it resulted in optimal energy use of the stance leg actuation.

There were differences in the exact shapes and the locations of the peak that should predict which value for K_p resulted in best disturbance rejection. For this model, these fixed points and these disturbance types, the actual disturbance rejection was best approached by GSN^{-1} .

Evaluation of the disturbance rejection results per transition type showed that there exists a wide range of combinations of push-off P and torque τ_{torso} that could result in a transition with good disturbance rejection, provided that the values for stiffness K_p and torque τ_{swing} were chosen correctly. This can be recognized in figure 8 where the results of the actual disturbance rejection are shown for every combination of push-off P and stiffness K_p . For all three types of transitions the white area, indicating the highest disturbance rejection, covers almost half of the

possible values for push-off P . When the value for push-off P is chosen, then the value for K_p and corresponding τ_{swing} that resulted in swing leg retraction showed the highest actual disturbance rejection. The size of the area of high disturbance rejection is bigger for the starting and slowing down transition than for the speeding up transition.

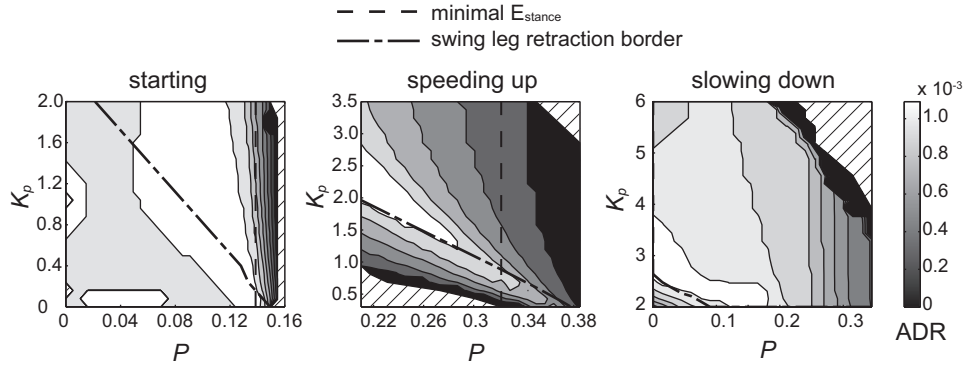


Fig. 8: Contourplots of actual disturbance rejection (ADR) for all combinations of push-off value P and spring stiffness K_p for the starting, speeding up and slowing down transitions; The vertical line indicates the optimal settings for P for energy use. Settings above the dash-dotted line result in swing leg retraction. The areas with highest actual disturbance rejection are white. Areas with a 45° hatch represent settings that do not result in a transition. Plot for stopping is not shown, because actual disturbance rejection is not computed for this transition.

Discrete LQR control applied to both the walking cycles as well as the transition step helped to increase the disturbance rejection properties even more. This is shown in figure 9 where the stiffness K_p is plot against the disturbance rejection measure for both the system without controller and with controller. The linear controller improved the disturbance rejection of the walker making a transition. It also shows that DLQR control enlarges the range of combinations of control input settings resulting in high disturbance rejection.

4. Discussion

We have shown that it is possible to change walking speed by making a dynamic one-step transition between two known fixed points without the need for multiple steps to converge to the new speed, even for big speed changes, and for starting and stopping. For every type of transition that was evaluated, the trade off is low between the optima in terms of energy use and disturbance rejection. The results from this research indicate that the versatility of dynamic walkers can be improved,

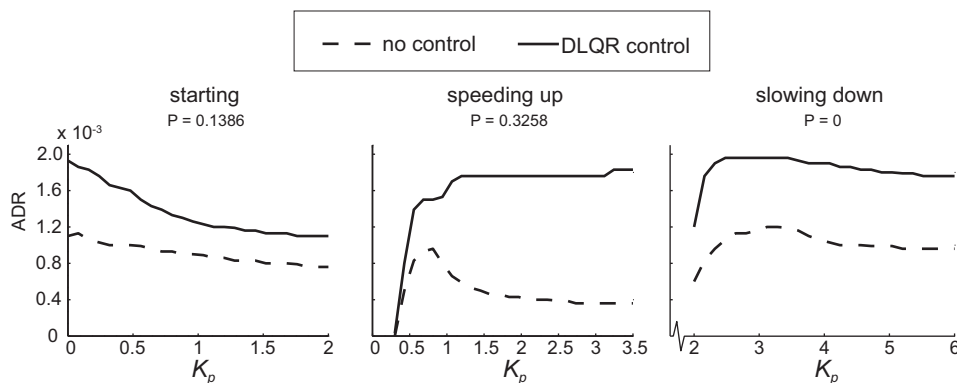


Fig. 9: Plots of stiffness K_p versus Actual disturbance for the starting, speeding up and slowing down transitions with and without DLQR control. For push-off P and τ_{torso} the energy use optimal settings were chosen.

while still exploiting advantages of dynamic walking.

To perform a transition with lowest energy use, energy is best to be added to the system by push-off, when the walking speed is to be increased. This also holds for starting up, whereas some torque around the torso is needed to initiate the rotational movement of stance-leg, which can not be done by a push-off. This fact that adding energy by push-off is cheaper than by a torque against a virtual torso has also been shown to hold for steady state walking⁹. In the case of a slow down or stopping transition, energy is to be dissipated. When the difference between the walking speed before and after the transition is too big to dissipate all superfluous energy during foot-strike only, then extra dissipation should be initiated by adding a negative torque around the torso. Since push-off can only add energy to the system, the slow down or stopping transition that uses no push-off uses minimal energy. For every type of transition it holds that the lowest possible spring stiffness and corresponding swing leg torque result in the lowest energy use for swing leg actuation.

It has been shown that a range of push-off values can be applied to make a transition, all resulting in high disturbance rejection, when appropriate values for the spring stiffness and the swing leg torque are chosen. The push-off value and corresponding torque around the torso that result in minimal energy use are within or close to this range. It turns out that good disturbance rejection highly depends on the swing leg movement and the choice for its actuators. The peak for maximal disturbance rejection is found for values of stiffness and torque around the swing leg that result in slight swing leg actuation, which is also true for steady state walking^{13,14}. Even though these are not the optimal values in terms of energy use, the trade-off is small. The maximal actual disturbance rejection for the speeding up

and slowing down transition is about 0.0012. This is between the values for actual disturbance rejection of slow steady state walking (0.0009) and fast steady state walking (0.0024), which means that performing a dynamic one-step transition does not make the system more sensitive to disturbances than steady state walking at the less stable of the two speeds. The disturbance rejection can even be increased by adding discrete optimal control to the transition and the walking cycles.

In our model we defined the swing leg actuation as two separate actuators, the spring and a constant torque. In some situations they are fighting against each other, both using energy. The two types of torque patterns could also be combined into one actuator, that describes a torque defined by two parameters, stiffness K_p and the constant torque τ_{swing} . This would have no difference in the prescribed trajectory and thus the transitions, but would have a positive effect on the energy use, which would decrease. Still it would hold that the lowest stiffness possible would result in the lowest energy use.

We compared several different targeting and robustness measures with the actual disturbance rejection and for our model, the chosen disturbance types and fixed points, the Gait Sensitivity Norm had the best correlation with the actual disturbance rejection, when comparing different settings to make the same transition. But to compare a transition between certain fixed points with another transition between other fixed points, the GSN can not be used, because to what extent the gait indicator differs from its nominal value gives no information about the maximal allowed deviation of the gait indicator. The targeting measures can not be used for such a comparison either, but the actual disturbance rejection can be used to compare such different transitions.

The simple 2D model with massless legs and little degrees of freedom is a highly simplified model, but there is no reason to believe that our strategy to transition would not work for more degrees of freedom in a 3D or real model. The advantage of using our simple walker model is that the trends on energy use and disturbance rejection are easy to distinguish. Whether these trends will also hold for more extensive models and even real prototypes has not been investigated, but is expected because the same trends as we found for transitions were shown to hold for steady state walking in both simple 2D models as well as in extended models.

We investigated transitions with pre-calculated control input values in one step and not for multiple steps. For certain transitions, like slowing down, it is likely to believe that they could be performed with even less energy use when the transition would take place during multiple steps, to dissipate all energy during foot-strike only, without actively performing negative work. The question in that case remains whether this also has a positive effect on the disturbance rejection or not.

A demand for the dynamic one-step transition strategy to work is that information is known about the goal states and the model. Experience in our lab has shown that the exact locations of fixed points and a precise model representation of a real prototype are not easy to obtain, due to the presence of many uncertainties. An analytical model of a prototype is needed to determine the location of fixed points and to find the control input values that result in the wanted transition. Even if an extensive model is not an exact representation of the real prototype, the found values can give a good indication of the needed settings.

In this study we apply the new dynamic one-step transition strategy to perform walking speed transitions. But actually it is a general strategy to make a step starting with some initial conditions, a location in phase space, and to end in another point in phase space. What the differences are between the two points in phase space should not matter for the transition and as a matter of fact they do not even have to be fixed points of limit cycles. These facts show that the dynamic one-step transition strategy has high potential for different applications only demanding that information is available about the current state and the desired states. This means that the same strategy could be applied to improve other aspects of versatility like changing direction while walking. And to improve robustness by application of the strategy as a non-linear controller during steady state walking, where it could be used to perform a one-step transition from the disturbed position in phase space back to the fixed point or from the fixed point to another location in phase space indicated by a path planner.

We did not study humans, but it might be that humans apply a similar strategy for transitions to change walking speed, where the needed control input values, the muscle forces, are obtained from experience and an internal model. Humans might apply the same optimization criteria of minimizing energy use, while maximizing the disturbance rejection, by applying the same trends as shown in this study.

We proposed a promising method to perform walking speed transitions by applying pre-calculated control input values to make a dynamic one-step transition. This method has been successfully applied to a simple powered walker model, which shows that the versatility of dynamic walkers can be improved. Performing transitions while still exploiting the natural dynamics of the system, allows us to keep the energy use and disturbance rejection at a level comparable to steady state walking.

References

1. Y. Sakagami, R. Watanabe, C. Aoyama, S. Matsunaga, N. Higaki and M. Fujita, The intelligent ASIMO: System overview and integration, in *Int. Conf. on Intelligent Robots and Systems 2002* **3** (2002) 2478–2483.
2. M. Vukobratovic, A. Frank, D. Juricic, On the stability of Biped Locomotion, *IEEE Transactions on Biomedical Engineering* **17**(1) (1970) 25–36.

3. T. McGeer, Passive Dynamic Walking, *International Journal of Robotics Research* **9**(2) (1990) 62–82.
4. S. Collins, A. Ruina, R. Tedrake, M. Wisse, Efficient Bipedal Robots Based on Passive-Dynamic Walkers *Science* **307**(5712) (2005), 1082–1085.
5. D. G. E. Hobbelen and M. Wisse, Limit cycle walking, in *Humanoid Robots, Human-Like Machines* ed. M. Hackel (I-Tech Education and Publishing, 2007), Chap. 14.
6. T. Mandersloot, M. Wisse and C.G. Atkeson, Controlling Velocity In Bipedal Walking: A Dynamic Programming Approach, in *6th IEEE-RAS Int. Conf. on Humanoid Robots* (IEEE Press, USA, 2006), pp.124–130.
7. D.G.E. Hobbelen and M. Wisse, Controlling the Walking Speed in Limit Cycle Walking, *International Journal of Robotics Research* **27**(9) (2008) 989–1005.
8. M. Garcia, A. Chatterjee, A. Ruina and M. Coleman, The Simplest Walking Model: Stability, Complexity, and Scaling, *ASME J. Biomech. Eng.* **120**(2) (1998) 281–288.
9. A.D. Kuo, Energetics of Actively Powered Locomotion Using the Simplest Walking Model, *ASME J. Biomech. Eng.* **124**(1) (2002) 113–120.
10. A. L. Hof, Scaling gait data to body size, *Gait & Posture* **4** (1996) 222–223.
11. G. Dean, An Analysis of the Energy Expenditure in Level and Grade Walking, *Ergonomics* **8** (1965) 31–47.
12. A.D. Kuo, A Simple Model of Bipedal Walking Predicts the Preferred Speed–Step Length Relationship, *ASME J. Biomech. Eng.* **123** (2001) 264–269.
13. M. Wisse, C.G. Atkeson and D.K. Kloimwieder, Swing leg retraction helps biped walking stability, in *5th IEEE-RAS Int. Conf. on Humanoid Robots* (IEEE Press, USA, 2005), pp.295–300.
14. D.G.E. Hobbelen and M. Wisse, Swing-Leg Retraction for Limit Cycle Walkers Improves Disturbance Rejection, *IEEE Transactions on Robotics* **24**(2) (2008) 377–389.
15. D.G.E. Hobbelen and M. Wisse, A Disturbance Rejection Measure for Limit Cycle Walkers: The Gait Sensitivity Norm, *IEEE Transactions on Robotics* **23** (2007) 1213–1224.